

Original

Effects of cleaning methods for custom abutment surfaces on gene expression of human gingival fibroblasts

Kazunori Nakajima¹⁾, Tetsuro Odatsu¹⁾, Ayano Shinohara¹⁾, Koumei Baba^{2,3)},
Yasuaki Shibata⁴⁾, and Takashi Sawase¹⁾

¹⁾Department of Applied Prosthodontics, Graduate School of Biomedical Sciences, Nagasaki University, Nagasaki, Japan

²⁾Industrial Technology Center of Nagasaki, Omura, Japan

³⁾Graduate School of Engineering, Nagasaki University, Nagasaki, Japan

⁴⁾Department of Histology and Cell Biology, Unit of Basic Medical Science, Graduate School of Biomedical Sciences, Nagasaki University, Nagasaki, Japan

(Received September 23, 2016; Accepted December 18, 2016)

Abstract: The aim of this study was to develop an effective method for cleaning implant abutments made by computer-aided design and computer-aided manufacturing techniques and to investigate the effect of decontamination *in vitro*. Briefly, a newly developed reagent (PK) and/or vacuum plasma (Plasma) were used to clean the surfaces of zirconia disks, and the effects of this decontamination were evaluated by X-ray photoelectron spectroscopy. Human gingival fibroblasts (HGFs) were cultured on sample disks for 6, 24, and 48 h. We evaluated cell attachment and gene expression of the acute inflammatory cytokines interleukin-6 and vascular endothelial growth factor A, and type 1 collagen. In the PK and PK+Plasma groups, surface contaminants were reduced by washing. In addition, HGF attachments was increased in the PK and PK+Plasma groups. Gene expressions of interleukin-6 and vascular endothelial growth factor A were lower at 6 h. Gene expression of type 1 collagen was increased at all time points after seeding. These results suggest that decontamination of implant abutment surfaces is important in initial

HGF attachment and may improve the biological seal of peri-implant soft tissue.

Keywords: decontamination; dental abutments; dental implants.

Introduction

Over the past several decades, the biocompatibility of dental implants has greatly improved clinical outcomes (1,2). Various approaches have been used to enhance osseointegration, such as control of surface topography with sandblasting, acid-etching, and hydroxyapatite coating (3-5). Rapid and secure osseointegration improves long-term outcomes (6,7), but several *in vitro* and animal studies have shown that adhesion of soft tissue to the dental abutment surface is required for long-term success, as it establishes an effective biological seal between soft tissue and the implant surface, thus limiting bacterial penetration, gingival recession, and bone recession (8).

Human gingival fibroblasts (HGFs) are an important component of connective tissue and are involved in homeostasis of collagen fibers around implant abutments. Moon et al. reported that connective tissue less than 40 μ m from implant abutments contained approx. 32% of the HGFs of all components. They concluded that HGFs help maintain the seal between soft tissue and implant abutments (9).

To satisfy the esthetic requirements of patients, an

Correspondence to Dr. Tetsuro Odatsu, Department of Applied Prosthodontics, Nagasaki University, Graduate School of Biomedical Sciences, 1-7-1 Sakamoto, Nagasaki 852-8588, Japan
Fax: +81-95-819-7689 E-mail: odatsu@nagasaki-u.ac.jp

doi.org/10.2334/josnusd.16-0681
DN/JST.JSTAGE/josnusd/16-0681

implant abutment should have an appropriate emergence profile for supporting peri-implant soft tissue (10,11). Because of their broad range of applications, customized implant abutments obtained by using computer-aided design and computer-aided manufacturing (CAD/CAM) techniques are now common. Titanium is the most widely used abutment material and has been very successful in long-term clinical practice (12). Yttrium-stabilized zirconia is used as an alternative material for implant abutments. Furthermore, a two-piece abutment—customized CAD/CAM zirconia coping cemented onto a prefabricated titanium base—is available in clinical practice (13).

Titanium and yttrium-stabilized zirconia are highly resistant to corrosion and have good biocompatibility (14,15). However, after milling with a CAD/CAM protocol and/or sintering with a furnace, customized abutments are manually adjusted and polished by a dental technician, except when a special modification is used for the titanium abutment surface (16,17). Because the abutment surface is contaminated with debris, several types of polishing materials, such as silicon points and diamond polishing paste, are used, in some cases by hand. Even CAD/CAM abutments with no manual adjustments in the lab exhibit contamination from the milling process (18). Canullo et al. reported that contaminants were present on abutment surfaces in contact with peri-implant tissue after the abutment was steam-cleaned (19). Other groups reported that debris or organic contamination from saliva remained even after cleaning by repeated ultrasonic washing with water, acetone, and ethanol (18,20). Such contamination, when present at the interface, may minimize soft-tissue adhesion and increase the risk of an inflammatory response in peri-implant tissues (21). Therefore, to maximize the inherent biocompatibility of titanium and zirconia, the abutment surface must be decontaminated before placement.

In this study, a cleaning protocol and vacuum plasma cleaning were used for decontamination. Organic and inorganic contaminants were removed with a newly developed solution containing protease and a surface activating agent. A plasma cleaning method was used in combination with the washing reagents. This dry-cleaning method is used in semiconductor manufacturing and removes organic contamination by breaking C-H and C-C bonds, which reduces surface-adsorbed hydrocarbon content (22).

Plasma cleaning methods are also used for surface modification. Plasma irradiation increases surface hydrophilicity by reducing the contact angle (23-25) and increases cell attachment to the irradiated surface.

Studies of the effects of decontamination investigated acute immune response by determining gene expressions of interleukin (IL)-6 and vascular endothelial growth factor A (VEGFA) (26,27). In addition, collagen type 1 (Col(I)- α 1) was evaluated to examine extracellular matrix (ECM) and collagen formation (28). The goals of the present study were 1) to develop a method for removing contaminants on CAD/CAM abutments after milling and possible manual modifications in the laboratory, and 2) to determine the effects of decontamination on HGF attachment and bioactivity.

Materials and Methods

Specimen preparation

Densely sintered zirconia ceramic disk-like specimens (Tosoh Corp., Tokyo, Japan) with a thickness of 1.7 mm and a diameter of 10.0 mm were used. A total of 68 disks were polished with 1,500-grit silicon carbide papers under water rinsing and then airborne-particle abraded with 50- μ m Al₂O₃ particles at a pressure of 2.5 bar for 15 s at a distance of 10 mm. The disks were then cleaned ultrasonically in a distilled water bath for 10 min (clean specimens). To simulate the manufacture of CAD/CAM abutments, the cleaned specimens were first contaminated with bare fingers, and then with polishing instruments using CeraMaster (Shofu, Kyoto, Japan) and diamond paste (Dia Glace, YETI Dentalprodukte, Engen, Germany), to standardize and imitate routine laboratory work (positive control).

A washing reagent (PK) was made from a protease solution containing 0.5% Proteinase K (Wako Pure Chemical Industries, Osaka, Japan), 5% Triton(R)-X (Nacalai Tesque, Kyoto, Japan), 5% sodium sulfite, and 0.01 M EDTA in 0.05 M Tris-HCl (pH 7.6). The specimens were divided into three experimental groups on the basis of the cleaning method used. PK group disks were washed with PK for 30 min and ultrasonically rinsed with distilled water for 10 min. Plasma group disks underwent a vacuum plasma protocol (YHS-R, Sakigake Semiconductor, Kyoto, Japan) for 10 min. PK+Plasma group disks were cleaned with vacuum plasma for 10 min after being treated with the PK reagent. A group without cleaning was used as a control group (Control).

To examine the effects of the cleaning methods, we used X-ray photoelectron spectroscopy (XPS) to determine the peak intensity of the carbon (C1s) spectrum of the disk surface. In addition, HGFs were cultured on disks in each test group, to determine associations between cell attachment, gene expression, and surface composition (Fig. 1).

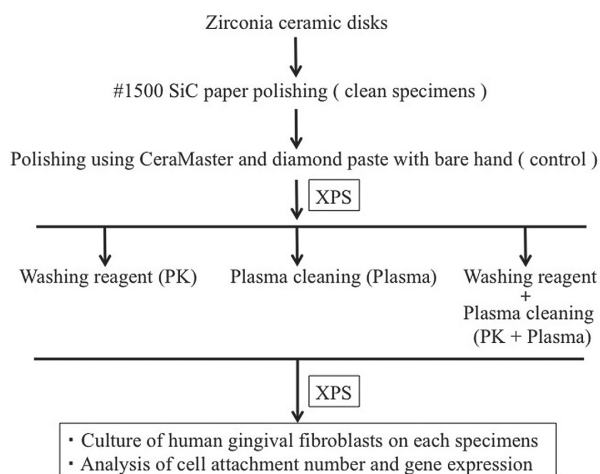


Fig. 1 Study design for chemical analysis and cell culture.

XPS analysis

To evaluate the composition of the outermost elements and the effects of the cleaning methods, we used an XPS system (ESCA 1000, Shimadzu, Kyoto, Japan) with argon sputtering at 2.0 kV and 20 mA for 95 min. High-resolution scans of the C1s, oxygen (O1s), zirconium (Zr3d), and nitrogen (N1s) peaks were obtained, and their relative compositions were calculated ($n = 3$).

Cell cultures

HGFs (a kind gift from Dr. Kazuma Takase, Department of Prosthetic Dentistry, Graduate School of Biomedical Sciences, Nagasaki University) were cultured in 150-cm² flasks with Dulbecco's modified Eagle's medium (D-MEM) containing 10% fetal bovine serum (FBS; Sigma-Aldrich, St. Louis, MO, USA) and antibiotics (1% penicillin/streptomycin) in a humidified atmosphere of 95% air and 5% CO₂ at 37°C. Cells from passages 3 and 4 were used in this study.

Cell attachment on disks

Polished disks were sterilized with ethylene oxide before cell culture. The cells were seeded on sample disks in 12-well plates (Nunc, ThermoFisher Scientific, Waltham, MA, USA) at a density of 100,000 cells per 1 mL of medium. After a 6-h incubation, the disks were twice washed with phosphate-buffered saline, to rinse unattached cells, and replaced on a fresh well plate. We used the MTS One Solution Assay (CellTiter 96, Promega, Madison, WI, USA) to measure the number of living cells in each well.

All treatments were exchanged with the cell proliferation assay treatment (D-MEM, 10% FBS, 1% penicillin/streptomycin, 317 $\mu\text{g mL}^{-1}$ MTS reagent, in accordance

with the manufacturer's protocol) and then incubated for an additional 4 h. To quantify cell numbers, we analyzed the color of the formazan product released by the cells with a spectrophotometer with a 490-nm filter (Multiskan FC, ThermoFisher Scientific) ($n = 5$).

Quantitative reverse transcriptase-polymerase chain reaction (qRT-PCR) assay

Cells on the zirconia disks ($n = 3$) in the control and treatment groups were lysed at each time point (6, 24, and 48 h after seeding), to collect mRNA (NucleoSpin RNA, Machery-Nagel, Dueren, Germany) and convert it to cDNA with reverse transcriptase (GoScript Reverse Transcription System, Promega), in accordance with the manufacturer's protocol. A microvolume UV-vis spectrophotometer (SimpliNano, GE Healthcare Life Sciences, Buckinghamshire, UK) was used to measure absorbance of mRNA and cDNA samples.

The details of the qRT-PCR assay were described previously (29). Briefly, using glyceraldehyde phosphate dehydrogenase (GAPDH) as an internal reference gene, we quantified relative gene expression with the comparative cycle threshold method, and fold change was calculated with the $2^{-\Delta\Delta\text{CT}}$ method. Data were normalized to GAPDH in each independent experiment and are expressed as relative induction of control at the corresponding time point.

Gene expressions of GAPDH and Col(I)- α 1 (6, 24, and 48 h after seeding) and VEGFA and IL-6 (at 6 h) were detected by a real-time PCR system (Thermal Cycler Dice, Takara Bio, Kusatsu, Japan) and with SYBR Green assay kits (SYBR Premix EX Taq II, Takara Bio). The sequences of all primers are listed in Table 1.

Data analysis and statistics

Data are presented as means \pm standard error. One-way analysis of variance (ANOVA) and the t -test were used for parametric analyses. A P value of <0.05 was considered to indicate statistical significance. All *in vitro* assays were repeated to ensure sufficient replicate sampling.

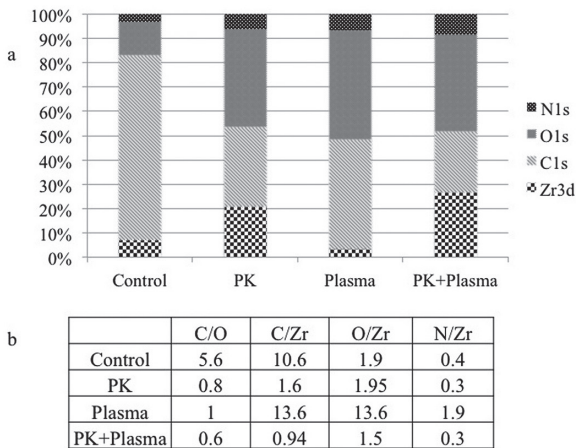
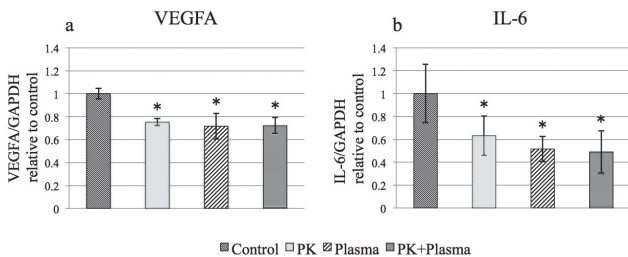
Results

XPS

Figure 2 shows the peak intensity ratios of C/O, C/Zr, O/Zr, and N/Zr in the three test groups. In the control group, the Zr3d ratio was $<10\%$ and mainly covered C1s. These results indicate that little of the Zr surface was exposed and that the disks were covered with coatings containing C1s, O1s, and N1s at the surface after routine lab work. The Zr3d ratio was higher in the PK and PK+Plasma groups, and the C1s ratio was lower. The Zr3d ratio in

Table 1 Primer sequences for the qRT-PCR assay

Gene	GenBank acc.	Sequences
GAPDH	NM_002046.5	Forward: GCACCGTCAAGGCTGAGAAC Reverse: TGGTGAAGACGCCAGTGG
Col(I)- α 1	NM_000088.3	Forward: GCTTGGTCCACTTGCTTGAAGA Reverse: GAGCATTGCCTTTGATTGCTG
IL-6	NM_000600.3	Forward: GCCAGAGCTGTGCAGATGAG Reverse: TCAGCAGGCTGGCATTG
VEGFA	NM_001025366.2	Forward: TCACAGGTACAGGGATGAGGACAC Reverse: CAAAGCACAGCAATGTCCTGAAG

**Fig. 2** X-ray photoelectron spectroscopic analysis of surface composition. a. Mean percentages for surface composition in each group. b. Mean ratios for carbon (C), oxygen (O), and nitrogen (N) in each group.**Fig. 4** Results of qRT-PCR analysis of human gingival fibroblasts after 6-h incubation on disks. a: VEGFA, b: IL-6. * $P < 0.05$.

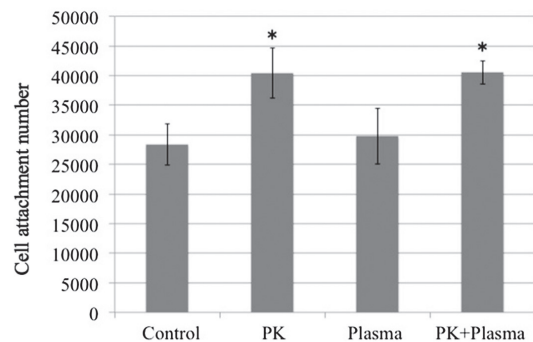
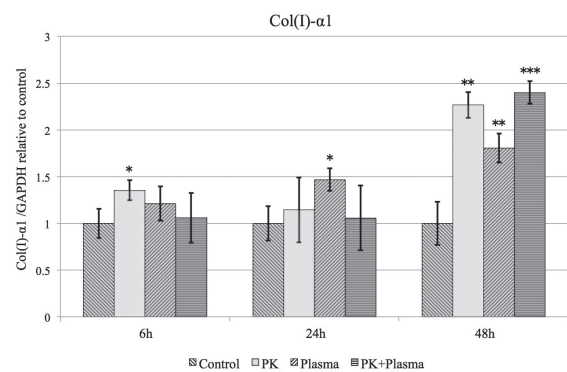
the Plasma group was similar to that in the control group.

Cell attachment on the samples

Figure 3 shows the number of attached cells in each sample group after 6 h of incubation. Cell numbers were significantly higher for the PK and PK+Plasma groups than for the control group.

Gene expression of fibroblasts

Gene expression of VEGFA was significantly lower after 6-h incubation in all washing groups (i.e., PK, Plasma,

**Fig. 3** Post-incubation cell attachment number in each group. * $P < 0.05$.**Fig. 5** Gene expression of Col(I)- α 1 after 6-, 24-, and 48-h incubation on disks. * $P < 0.05$, ** $P < 0.01$, *** $P < 0.005$.

and PK+Plasma) (Fig. 4a), and gene expression of IL-6 was lower at 6 h in all washing groups (Fig. 4b). Gene expression of Col(I)- α 1 was significantly higher at 6 h in the PK groups and at 24 h in the Plasma group. It was markedly increased in all washing groups at 48 h (Fig. 5).

Discussion

The aims of the present study were to develop a method to remove contaminants on CAD/CAM abutments from milling and possible manual modifications in the laboratory and to investigate the effects of decontamina-

tion on HGF attachment and bioactivity. XPS analysis showed that organic coatings mainly comprised carbon (C), oxygen (O), and nitrogen (N) on ceramic materials, which were detected as the peak intensity of C1s, O1s, and N1s (30). In addition, C/Zr, O/Zr, and N/Zr ratios in the control group tended to be higher than those in the test groups, which confirmed the presence of organic contamination.

C/Zr, O/Zr, and N/Zr ratios were lower in the PK and PK+Plasma groups than in the control group, which suggests that organic contamination was washed out and that the solid Zr surface was exposed. The C1s ratio decreased in the Plasma group, but increases in the O1s and N1s ratios resulted in less exposure of the Zr surface. Thus, PK is essential for removing organic coatings on a Zr surface, which was contaminated by laboratory manipulation. In contrast, the cleaning effect of plasma irrigation was limited, as the plasma could not penetrate the thick organic coating.

Initial cell attachment involves a number of complex steps, which ensure binding of membrane proteins to the ECM, intracellular cytoskeleton formation, and signal transduction (31,32). It was reported that focal adhesion molecules such as focal adhesion kinase (33-35), vinculin (28), and integrin (36,37) have roles in gingival fibroblast attachment on an abutment surface, but the underlying mechanisms are unclear. Therefore, we used an MTS assay to evaluate cell attachment on specimen surfaces. In this study, cell attachment number on disks was higher at 6 h after cell seeding in the PK and PK+Plasma groups but not in the Plasma group. These results indicate that PK treatment is not cytotoxic and that it promotes cell attachment to CAD/CAM abutments after milling and manual handling in the laboratory.

Col(I)- α 1 is an ECM produced by HGFs and is the main component of collagen in soft tissues around implants. An increase in Col(I)- α 1 gene expression may lead to HGF attachment and synthesis of collagen-rich connective tissue. This may yield a tighter seal around the abutment, thus avoiding bacterial penetration and growth of gingival epithelial cells and facilitating wound healing repair and regeneration (38,39).

IL-6 is a pleiotropic cytokine with varied biological activities, such as induction of acute immune reaction, regulation of immune responses, and promotion of hematopoiesis (26). IL-6 is also an important osteotropic cytokine involved in osteoclast differentiation and bone-resorption regulation mechanisms (40). VEGFA is a growth factor in neovascularization. It is important in angiogenesis and can enhance the inflammatory response through its effects on vascular permeability. VEGFA

expression is induced by several inflammatory cytokines, including IL-6 (27). In the present study, gene expressions of VEGFA and IL-6 at 6 h were significantly lower in the test groups (PK, Plasma, and PK+PL) than in the control group. In contrast, gene expression of Col(I)- α 1 at 48 h was significantly higher in the test groups than in the control group.

Inflammatory events involve a series of complex interactions between enzymatic and non-enzymatic mechanisms, including synthesis of reactive oxygen species, pro-inflammatory cytokines, and matrix metalloproteinases. Cavalla et al. reported that IL-6 and VEGF expressions of human periodontal ligament fibroblast in oxidative stress model were higher than in non-oxidative stress model (41). Matsui et al. reported that reactive oxygen species inhibited production of type I collagen mRNA and collagen protein in 24- and 72-h HGF cultures (42). We hypothesize that the present decreases in IL-6 and VEGFA expressions at 6 h resulted in the increase in Col(I)- α 1 expression at 48 h.

Our results suggest that decontamination of an implant abutment after laboratory work enhances abutment biocompatibility and prevents inflammation of peri-implant tissue. The implant-abutment interface is close to the bone. Abutment decontamination may thus help suppress bone resorption around the implant platform.

The efficiency of decontamination was better for the washing reagent and the combination of washing reagent and vacuum plasma than for plasma alone. The decontaminated zirconia surface enhanced HGF cell attachment, reduced the inflammatory cytokine level, and promoted collagen gene expression. Despite the positive outcomes of this *in vitro* study and the preliminary clinical results, clinical and histological studies should be conducted to confirm whether the improved fibroblast adhesion decontaminated by PK and/or plasma improves formation of collagenous connective tissue, thus preventing short-, medium-, and long-term peri-implantitis.

Acknowledgments

We thank Dr. Kazuma Takase (Nagasaki University) for providing human fibroblasts. This work was supported by JSPS KAKENHI Grant No. 24792146.

Conflict of interest

None declared.

References

1. Cook SD, Dalton JE (1992) Biocompatibility and biofunctionality of implanted materials. *Alpha Omegan* 85, 41-47.
2. Steflik DE, Corpe RS, Young TR, Buttle K (1998) *In vivo*

- evaluation of the biocompatibility of implanted biomaterials: morphology of the implant-tissue interactions. *Implant Dent* 7, 338-350.
3. Grill V, Sandrucci MA, Rizzo R, Narducci P, Bareggi R, Dorigo E (2000) Biocompatibility in vitro of titanium dental implants. Immunocytochemical expression of fibronectin and extracellular matrix receptors. *Minerva Stomatol* 49, 77-85.
 4. Li D, Liu B, Han Y, Xu K (2001) Effects of a modified sandblasting surface treatment on topographic and chemical properties of titanium surface. *Implant Dent* 10, 59-64.
 5. Meirelles L, Albrektsson T, Kjellin P, Arvidsson A, Franke-Stenport V, Andersson M et al. (2008) Bone reaction to nano hydroxyapatite modified titanium implants placed in a gap-healing model. *J Biomed Mater Res A* 87, 624-631.
 6. Le Guéhennec L, Soueidan A, Layrolle P, Amouriq Y (2007) Surface treatments of titanium dental implants for rapid osseointegration. *Dent Mater* 23, 844-854.
 7. Simion M, Benigni M, Al-Hezaimi K, Kim DM (2015) Early bone formation adjacent to oxidized and machined implant surfaces: a histologic study. *Int J Periodontics Restorative Dent* 35, 9-17.
 8. Rompen E, Domken O, Degidi M, Pontes AE, Piattelli A (2006) The effect of material characteristics, of surface topography and of implant components and connections on soft tissue integration: a literature review. *Clin Oral Implants Res* 17, Suppl 2, 55-67.
 9. Moon IS, Berglundh T, Abrahamsson I, Linder E, Lindhe J (1999) The barrier between the keratinized mucosa and the dental implant. An experimental study in the dog. *J Clin Periodontol* 26, 658-663.
 10. Glauser R, Sailer I, Wohlwend A, Studer S, Schibli M, Schärer P (2004) Experimental zirconia abutments for implant-supported single-tooth restorations in esthetically demanding regions: 4-year results of a prospective clinical study. *Int J Prosthodont* 17, 285-290.
 11. Kutkut A, Abu-Hammad O, Mitchell R (2015) Esthetic considerations for reconstructing implant emergence profile using titanium and zirconia custom implant abutments: fifty case series report. *J Oral Implantol* 41, 554-561.
 12. Park JM, Lee JB, Heo SJ, Park EJ (2014) A comparative study of gold UCLA-type and CAD/CAM titanium implant abutments. *J Adv Prosthodont* 6, 46-52.
 13. Gehrke P, Alius J, Fischer C, Erdelt KJ, Beuer F (2014) Retentive strength of two-piece CAD/CAM zirconia implant abutments. *Clin Implant Dent Relat Res* 16, 920-925.
 14. Smith DC (1993) Dental implants: materials and design considerations. *Int J Prosthodont* 6, 106-117.
 15. Sennerby L, Dasmah A, Larsson B, Iverhed M (2005) Bone tissue responses to surface-modified zirconia implants: a histomorphometric and removal torque study in the rabbit. *Clin Implant Dent Relat Res* 7, Suppl 1, S13-S20.
 16. Nevins M, Nevins M, Gobbato L, Lee HJ, Wang CW, Kim DM (2013) Maintaining interimplant crestal bone height via a combined platform-switched, Laser-Lok implant/abutment system: a proof-of-principle canine study. *Int J Periodontics Restorative Dent* 33, 261-267.
 17. Kim YS, Ko Y, Kye SB, Yang SM (2014) Human gingival fibroblast (HGF-1) attachment and proliferation on several abutment materials with various colors. *Int J Oral Maxillofac Implants* 29, 969-975.
 18. Gehrke P, Tabellion A, Fischer C (2015) Microscopical and chemical surface characterization of CAD/CAM zirconia abutments after different cleaning procedures. A qualitative analysis. *J Adv Prosthodont* 7, 151-159.
 19. Canullo L, Micarelli C, Iannello G (2013) Microscopical and chemical surface characterization of the gingival portion and connection of an internal hexagon abutment before and after different technical stages of preparation. *Clin Oral Implants Res* 24, 606-611.
 20. Yang B, Scharnberg M, Wolfart S, Quaas AC, Ludwig K, Adelung R et al. (2007) Influence of contamination on bonding to zirconia ceramic. *J Biomed Mater Res B Appl Biomater* 81, 283-290.
 21. Mishra PK, Wu W, Rozo C, Hallab NJ, Benevenia J, Gause WC (2011) Micrometer-sized titanium particles can induce potent Th2-type responses through TLR4-independent pathways. *J Immunol* 187, 6491-6498.
 22. Amaral R, Ozcan M, Bottino MA, Valandro LF (2006) Microtensile bond strength of a resin cement to glass infiltrated zirconia-reinforced ceramic: the effect of surface conditioning. *Dent Mater* 22, 283-290.
 23. Valverde GB, Coelho PG, Janal MN, Lorenzoni FC, Carvalho RM, Thompson VP et al. (2013) Surface characterisation and bonding of Y-TZP following non-thermal plasma treatment. *J Dent* 41, 51-59.
 24. Kobune K, Miura T, Sato T, Yotsuya M, Yoshinari M (2014) Influence of plasma and ultraviolet treatment of zirconia on initial attachment of human oral keratinocytes: expressions of laminin γ_2 and integrin β_4 . *Dent Mater J* 33, 696-704.
 25. Noro A, Kameyama A, Haruyama A, Takahashi T (2015) Influence of hydrophilic pre-treatment on resin bonding to zirconia ceramics. *Bull Tokyo Dent Coll* 56, 33-39.
 26. Akira S, Taga T, Kishimoto T (1993) Interleukin-6 in biology and medicine. *Adv Immunol* 54, 1-78.
 27. Cohen T, Nahari D, Cerem LW, Neufeld G, Levi BZ (1996) Interleukin 6 induces the expression of vascular endothelial growth factor. *J Biol Chem* 271, 736-741.
 28. Guillem-Marti J, Delgado L, Godoy-Gallardo M, Pegueroles M, Herrero M, Gil FJ (2013) Fibroblast adhesion and activation onto micro-machined titanium surfaces. *Clin Oral Implants Res* 24, 770-780.
 29. Qiu H, Durand K, Rabinovitch-Chable H, Rigaud M, Gazaille V, Clavère P et al. (2007) Gene expression of HIF-1 α and XRCC4 measured in human samples by real-time RT-PCR using the sigmoidal curve-fitting method. *BioTechniques* 42, 355-362.
 30. Kwon YD, Choi HJ, Lee H, Lee JW, Weber HP, Pae A (2014) Cellular viability and genetic expression of human gingival fibroblasts to zirconia with enamel matrix derivative (Emdogain®). *J Adv Prosthodont* 6, 406-414.

31. Akiyama SK (1996) Integrins in cell adhesion and signaling. *Hum cell* 9, 181-186.
32. Gumbiner BM (2000) Regulation of cadherin adhesive activity. *J Cell Biol* 148, 399-404.
33. Burridge K, Chrzanowska-Wodnicka M (1996) Focal adhesions, contractility, and signaling. *Annu Rev Cell Dev Biol* 12, 463-518.
34. Schaller MD, Hildebrand JD, Parsons JT (1999) Complex formation with focal adhesion kinase: a mechanism to regulate activity and subcellular localization of Src kinases. *Mol Biol Cell* 10, 3489-3505.
35. Hanks SK, Ryzhova L, Shin NY, Brábek J (2003) Focal adhesion kinase signaling activities and their implications in the control of cell survival and motility. *Front Biosci* 8, d982-996.
36. Yamano S, Ma AK, Shanti RM, Kim SW, Wada K, Sukotjo C (2011) The influence of different implant materials on human gingival fibroblast morphology, proliferation, and gene expression. *Int J Oral Maxillofac Implants* 26, 1247-1255.
37. Gómez-Florit M, Xing R, Ramis JM, Taxt-Lamolle S, Haugen HJ, Lyngstadaas SP et al. (2014) Human gingival fibroblasts function is stimulated on machined hydroxylated titanium zirconium dental implants. *J Dent* 42, 30-38.
38. Bartold PM, Walsh LJ, Narayanan AS (2000) Molecular and cell biology of the gingiva. *Periodontol* 24, 28-55.
39. Abiko Y, Hiratsuka K, Kiyama-Kishikawa M, Tsushima K, Ohta M, Sasahara H (2004) Profiling of differentially expressed genes in human gingival epithelial cells and fibroblasts by DNA microarray. *J Oral Sci* 46, 19-24.
40. Theoleyre S, Wittrant Y, Tat SK, Fortun Y, Redini F, Heymann D (2004) The molecular triad OPG/RANK/RANKL: involvement in the orchestration of pathophysiological bone remodeling. *Cytokine Growth Factor Rev* 15, 457-475.
41. Cavalla F, Osorio C, Paredes R, Valenzuela MA, García-Sesnich J, Sorsa T et al. (2015) Matrix metalloproteinases regulate extracellular levels of SDF-1/CXCL12, IL-6 and VEGF in hydrogen peroxide-stimulated human periodontal ligament fibroblasts. *Cytokine* 73, 114-121.
42. Matsui S, Tsujimoto Y, Ozawa T, Matsushima K (2011) Antioxidant effects of antioxidant biofactor on reactive oxygen species in human gingival fibroblasts. *J Clin Biochem Nutr* 48, 209-213.